ON THE APPLICATION OF BAYESIAN INFERENCE FOR AXIAL COMPRESSOR PERFORMANCE ASSESSMENT

Gonçalo G. Cruz
von Karman Institute for Fluid Dynamics
Rhode-St-Genèse, Belgium

Fabrizio Fontaneto
von Karman Institute for Fluid Dynamics
Rhode-St-Genèse, Belgium

ABSTRACT

Reducing the instrumentation required to evaluate the performance of a turbomachine is essential to reduce intrusiveness error and to limit the cost of a measurement campaign. A data assimilation methodology based on Bayesian Inference is employed to reduce the required instrumentation effort. A numerical model is employed to provide an initial belief of the flow, that is then updated based on experimental observations. The developed methodology has been validated on analytical cases on which a thorough parametric study was also performed. Preliminary results on a low aspect ratio axial compressor stage show a good prediction of the corrected compressor map, as well as a good prediction of the inter-row pressure ratio of the machine.

INTRODUCTION

With the trend of achieving higher pressure ratios, more compact machines are being designed, making turbomachinery components more sensitive to instrument intrusiveness in the flow.

Non-intrusive experimental techniques, such as Particle Image Velocimetry (PIV) and Laser Doppler Velocimetry (LDV) are not easy to apply to turbomachines and are not of direct implementation in the industry. Probe intrusiveness in turbomachinery flows has been researched to assess the impact of the measurements on the aerodynamic design of the machines. Research has been conducted both in compressors (Sanders et al., 2017), where Computational Fluid Dynamics (CFD) calculations show a probe influence on the wake leading to differences in the aerodynamic excitation, and turbines (Aschenbruck et al., 2015), where the probes reduce the wake magnitude in areas with high velocity gradients. Validation of CFD simulations with the use of multi-hole pressure probes that disturb the flow field becomes a issue to be wary upon.

With this in mind, research and development of less intrusive experimental techniques is required to reduce the number of probes used throughout the machine and consequently diminish the influence of measurements in the flow, while maintaining high fidelity results, and reducing the costs associated with probes.

Parallel to this need, an increased interest in data assimilation algorithms and their applications in fluid mechanics has been noticed. Their main advantage lies in the capability of coupling experimental measurements with numerical models. Particularly interesting, is the utilization of data assimilation with Bayesian inference applied to inverse problems beyond meteorological forecast and oceanography (Bannister, 2017).

This trend towards data science provides the perfect opportunity to study a new approach to tackle probe intrusiveness in the flow field of a turbomachine, by developing of a new hybrid, less intrusive experimental technique, that employs data assimilation. This paper sets out to investigate the feasibility of data assimilation with Bayesian inference on a state-of-the-art compressor stage, which due to its blade height is affected by probe intrusiveness, by evaluating its global performance.

Data assimilation performed with Bayesian inference combines all available knowledge about the studied system, where the available information is evaluated with probability functions (Dwight, 2014). These methods are equivalent to solving a maximum likelihood estimate problem based on the Bayes theorem, which can be written as:

$$P(Model|Data) = \frac{P(Data|Model) \cdot P(Model)}{P(Data)}$$

where $P(Data|Model)$ is called likelihood, matching both measured data and forward model in this case. The likelihood is estimated using a Bayesian inference method that is to be chosen and discussed below.

$P(Model)$ is the prior distribution, in this case given by the forward model presented in the next section. This member of the equation represents the *priori* belief of the distribution of a certain quantity of interest.

$P(Data)$ is the marginal likelihood. It is constant, since it is independent of the forward model used, being sometimes omitted from the formula, since it is meant to normalize the obtained pdf.

$P(Model|Data)$ is the posterior distribution, the result of the application of the data assimilation procedure with a Bayesian inference algorithm. This result is the *posteriori*, the updated belief, based on forward model and observed data.

A Bayesian inference method is required. Various methods and consequent sub-variations are found in the literature: The Ensemble Kalman Filter (EnKF) (Evensen, 2003, 2010; Stordal et al., 2011), the Markov Chain Monte Carlo (MCMC) (Apte et al., 2007; Wikle & Berliner, 2007) and variational methods, in particular, the 4D-VAR (Jardak et al., 2010; Lorenc, 2003; Penenko, 2009).

The adaption of the EnKF for inverse problems (Iglesias, Law, & Stuart, 2013) was chosen for its simple formulation, which leads to a straightforward implementation. The fact that this method is gradient-free reduces the computational cost of the data assimilation process. The data assimilation update step is computed without a need to compute gradients, making it cost-effective when compared with gradient based methods. The downside of the algorithm, lies on the assumption that all the probability distributions are Gaussian, which is acceptable since literature shows that the algorithm can still provide acceptable results for other distributions (Sousa, García-Sánchez, & Gorlé, 2018).

The following sections of the present work include an introduction to the compressor stage test case of this work, followed by a thorough description of the proposed methodology, with special attention to the description of the Bayesian inference algorithm employed. The results show the capability of the methodology to predict within a confidence level the machine operating condition. Arguments towards the present approach are taken and conclusions are drawn about the possibility of the method to reduce the number of experimental measurements required to fully characterize the compressor stage.

TEST CASE – H25 COMPRESSOR STAGE

The test case of this paper is the LEMCOTEC H25 test section. It is a single stage axial compressor designed to represent the last stage of a high pressure compressor for a high overall pressure ratio engine, being characterized by its low aspect ratio blade design with a blade height of 25 mm, achieving a total-to-total pressure ratio of 1.25 at design conditions.

A cross section of the experimental setup of H25 stage is shown in Figure 1. Combined total pressure - total temperature rakes are deployed at measurement Planes 0 and 4, that correspond, respectively to the inlet and outlet of the compressor stage, allowing the assessment of the stage overall performance. Radial measurements are taken with a transverse probe in all measurement planes at constant throttle, being 27 measurements taken in each profile. Azimuthal traversing is only possible in Plane 4. VKI 3-hole pneumatic pressure probes resolve the span-wise total pressure distribution and blade-to-blade flow angle. Static pressure taps are present, both at the hub and casing, in all measurement planes.

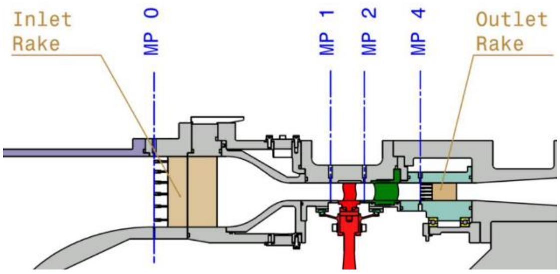

Figure 1 - Cut - View of the LEMCOTEC H25 Test Section

The fully propagated total and static pressure uncertainties are, in the worst-case scenario (Plane 0), equal to 3.2% and 3% of the dynamic pressure respectively. The total temperature uncertainty was computed to be equal 2.5% of the total temperature ratio. The total-to-total pressure ratio related uncertainty budget was estimated to be lower than 1% while the mass flow and the isentropic efficiency uncertainties are equal to 2.1% and 4% for a near-stall operating condition.

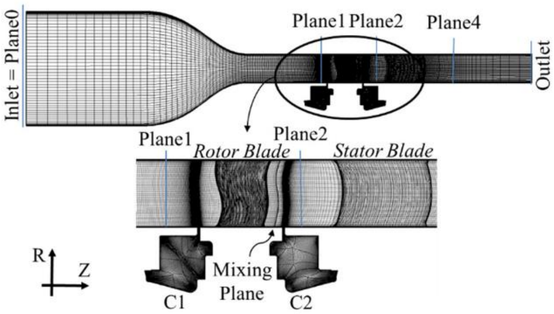

Figure 2 - H25 Stage Meridional View of the Numerical Domain

Coupled with the vast experimental data described, a CFD model of the compressor domain has been developed and thoroughly validated (Babin et al, 2020) Figure 2 shows the numerical domain of the stage, defined from Plane 0, the inlet test section, to two rotor mid-span chords downstream of Plane 4, the outlet of the test section. A mixing plane approach is applied to link rotor and stator.

A multi-block structured mesh approach is chosen. The O-4H mesh topology is used for both rotor and stator rows while the rotor tip gap region is meshed with O-H topology. Three mesh levels were developed, a coarse, a medium and a finer one, with, respectively, 0.5 million, 3.6 million and 28 million surface domain cells.

Fully turbulent RANS computations coupled with the k-ω SST turbulence model (Menter, 1994) are run. Experimental measurements are used to define the domain boundary conditions. At the inlet, the measured total quantities distributions are employed along with the flow angle. At the outlet, for this work in specific, a constant mass flow value, measured in a working point of interest was imposed to force the flow field to adapt to different inlet total conditions variation.

METHODOLOGY

The objective of the proposed methodology comprises in the reduction of the instrumentation required to characterize a turbomachine, relying on a data assimilation framework to infer the flow field across the studied machine and its working conditions. Figure 3 shows a schematic of the proposed methodology which relies on three main building blocks, a forward model, an experimental database, and a Bayesian inference algorithm, in this case, the ensemble Kalman filter. The methodology can be summarized as it follows:

1. An ensemble is sampled from a prior belief (initial guess) about the inlet total pressure probability distribution at which the machine is operating.
2. Using computational fluid dynamics as a model, compute the quantities of interest of the compressor flow field for each ensemble member.
3. Compare the obtained flow fields against randomly selected experimental data and use the Bayesian inference algorithm to update the propagated ensemble flow fields and the initial belief of the inlet total pressure.
4. Validate the updated flow field against experimental measurements not used in the previous data assimilation step.

The pressure in the test rig of the compressor stage is usually equal to the atmospheric pressure but it can be changed to control the Reynolds number at which the machine operates. Throughout the year and even throughout the day, atmospheric conditions vary and can affect the experimental campaign. With this in mind, the definition of the prior belief of the inlet total pressure is taken to be an uniform distribution around a mean atmospheric pressure, $p_0/p_{atm} \sim \mathcal{U}(0.85,1.15)$.

The selection of such a weakly informative prior distribution avoids biasing the algorithm, while ensuring the regularization of it, since the selected prior is bounded to the truth (Zhang, Michelén-Ströfer, & Xiao, 2019), avoiding the problem to become ill-posed.

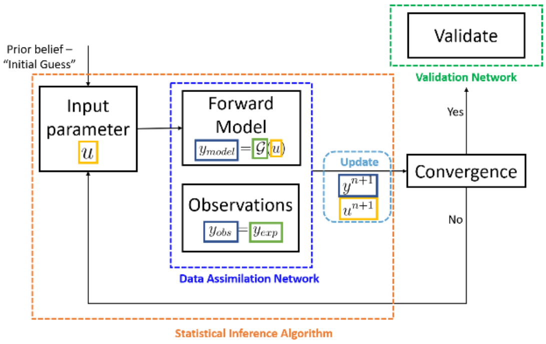

Figure 3 - Methodology schematic

The use of a forward model is required. This model can be a dynamic model (Sakov & Oke, 2008), surrogate models (Marzouk & Najm, 2009) or a Computational Fluid Dynamics (CFD) computation, the latter being the approach chosen for this work, due to its higher level of fidelity, allowing a stronger proof of concept for the methodology.

25 CFD runs were performed, in the medium mesh, instead of the finest one with the aim of reducing computational cost. A baseline case was run in the finer mesh and compared against the same case, obtained in the medium mesh, being the difference between results used to estimate the model error distribution. The values for the input total inlet pressure were randomly sampled from the above presented prior belief uniform distribution. Of the 25 randomly sampled inlet total pressures, two of them, which correspond to low pressure values, failed to converge due to the back pressure imposed by the mass flow outlet boundary condition.

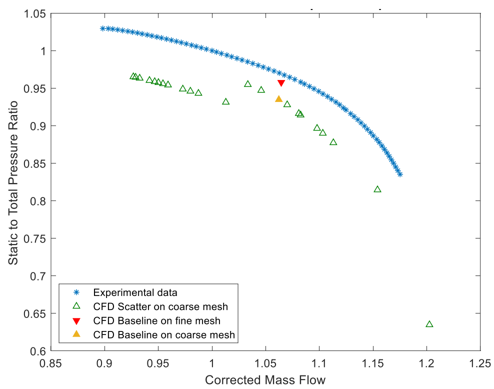

Figure 4 - Normalized Corrected Compressor Map

Parallel to this, an experimental database of the compressor stage is available. The results obtained from the CFD model runs and the experimental database allow the computation of the machine compressor maps, presented in Figure *4* with corrected mass flow against static to total pressure ratio. It is clearly noticeable the difference between the experimental and the numerical compressor maps. The CFD medium mesh, clearly shows an offset relative to the experimental data, underestimating the static to total pressure ratio of the stage, being this offset higher towards the stall region.

The last building block of the methodology is the statistical inference algorithm, the EnFK for inverse problems (Iglesias et al., 2013). It assimilates experimental measurements (y) with the CFD flow field results ($\mathcal{G}(u)$) to update the working point (u) and the flow field of the machine.

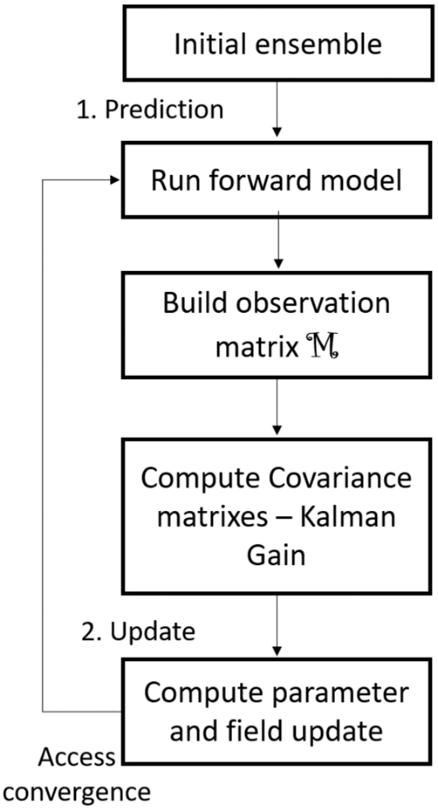

Figure 5 - Algorithm Schematic

The experimental data has an associated probability distribution due to noisy measurements (y). The compressor stage flow field ($\mathcal{G}(u)$) will also show fluctuations with respect to the inlet conditions (u). Therefore, when performing the data assimilation update step, we are interested in retrieving a well-defined probability density function and not just a mean value, which is exactly what is achieved by using Bayesian approach. The steps of the algorithm are schemed in Figure *5* and summarized as it follows based on (Sousa & Gorlé, 2019):

From the selected prior distribution initial guess, u, an initial ensemble of size J, $u_{j=,\dots,J}$, is sampled from random draws of the prior distribution around a mean with a known covariance, C_{uu}.

The ensemble, u, is then propagated as the input of the forward non-linear model, $\hat{\mathcal{G}}(\mathrm{u})$, that added to a given model error, q, provides a field vector, Φ, that represents the complete domain output of the model.

$$\Phi_j(x) = \hat{\mathcal{G}}(u_j) + q_j(x)$$

To apply the EnKF update step, observations, y, are required. These are experimental measurements which have a known associated uncertainty and therefore a known covariance, $C_{\epsilon\epsilon}$, and are independent of the iteration process.

Since these observations are only available in $\mathcal{M}$ positions along the domain, a measurement matrix is applied to the field vector to obtain $\hat{\mathrm{d}}$, which contains the field vector, Φ, only at the location of the observations.

$$\hat{d}_j = \mathcal{M}\left[\Phi_j(x)\right]$$

From the initial generated ensemble, which represents a first guess, the iterative process uses the ensemble, u, to predict the field vector, Φ, and sub sequentially build $\hat{d}$, which is updated with a combined weight between the model and observed states, represented by the Kalman gain.

The update of the initial parameter and field vector are performed with the usage of covariance matrices that relate the initial ensemble with the propagated field forecast and can be found in (Sousa & Gorlé, 2019).

The updated parameter distribution becomes then the new ensemble to propagate in the model and the process is repeated for a fixed number of iterations, on which convergence is assessed. After convergence, the updated field vector is processed in a validation network where is compared to independent experimental observations.

The algorithm performance will be evaluated in this work with usage of the mean absolute error (MAE) between the updated result and a reference solution for each domain point.

$$\mathrm{MAE} = \frac{1}{J}\sum_{j=1}^{J}\left|\Phi_j - y_j^{truth}\right|$$

To close the methodology, and before applying it to the H25 compressor stage, the algorithm needs to be validated. Adding to it, algorithm parameters, such as the number of ensemble members, J, are user defined, being a sensitivity analysis required to evaluate their impact on the algorithm performance.

The Lorenz system (Lorenz, 1963) is selected as the validation case for the current approach due to its non-linear, chaotic behaviour, while being deterministic. It is defined by the following system of equations:

$$\frac{\mathrm{d}x}{\mathrm{d}t} = \sigma(y - x)$$

$$\frac{\mathrm{d}y}{\mathrm{d}t} = x(\rho - z) - y$$

$$\frac{\mathrm{d}z}{\mathrm{d}t} = xy - \beta z$$

with $\rho = 28$, $\sigma = 10$ and $\beta = 8/3$, ensuring the system to present chaotic behaviour. Artificial data can be generated with the usage of a 4th order Runge-Kutta method. The system has been widely studied in the literature and in this work, the algorithm will focus on inferring the starting boundary conditions, $(x_0, y_0, z_0) = (10,20,30)$, based on artificially generated model runs with added error and noisy experimental data sampled randomly along a fixed time domain.

A first run of the algorithm on the Lorenz system showed promise in the approach, despite presenting a higher error than the classic EnKF (Evensen, 2003) for the same number of ensemble members but still giving a reliable posterior result for the system boundary conditions. This result still validates the algorithm implementation and a parametric study was run where attention was given to the ensemble size, J.

As mentioned in the literature, it was verified that an increase in the ensemble size leads to a decrease in the obtained error, being this a trade-off since a higher number of ensemble members means a higher computational cost of the algorithm. An algorithm run is performed with an ensemble size, J = 1000. The model error, q, is set to $q \sim \mathcal{N}(0,0.1)$. Experimental observations, y, are artificially created in half of the time steps evaluated by the model run. These observations have an artificial added white noise of the form $\eta \sim \mathcal{N}(0,1)$. The prior distribution for the starting positions, (x_0, y_0, z_0), is chosen to be a uniform distribution with bounds set to ± 3 the "truth" position mentioned above. In these conditions the obtained posteriors, for one iteration of the algorithm with a random seed, are summarized in Table 1.

Table 1 - Lorenz system posterior update

Position	Truth	Prior	Posterior
x_0	10	$\mathcal{U}(7,13)$	$\mathcal{N}(9.43,0.82)$
y_0	20	$\mathcal{U}(17,23)$	$\mathcal{N}(19.7,0.30)$
z_0	30	$\mathcal{U}(27,33)$	$\mathcal{N}(29.2,1.01)$

The algorithm is clearly able to retrieve the truth about the starting position from a wide uniform distribution. Adding to it, the mean MAE of the updated obtained field is around 0.6, which is a very acceptable result when dealing with a non-linear, chaotic system. The just presented analysis validates the algorithm implementation. Despite that, another validation case was tested.

The Rankine vortex (Ide & Ghil, 1998) is a very organized, simple theoretical case, which results from the interaction between a free and a forced vortex and its highly dependent on the vortex constants. Summarizing, the algorithm was able to retrieve the velocity magnitude along the radius of the vortex, as well as, the vortex constant parameter with good accuracy, using a reduced ensemble size, J = 30. This shows how the complexity of the problem being solved changes the required number of ensemble members.

A parallelism can be established. The test case of this work, the H25 compressor stage, is expected to be between these two validation cases, not being as chaotic and ill-posed as the Lorenz system but not being organized as the Rankine vortex.

RESULTS AND DISCUSSION

Throughout this section, the results obtained with the proposed methodology are presented and discussed, on a 1D mean pressure approach, which allows the inference of the machine compressor map.

As previously mentioned, from a prior uniform distribution around the atmospheric pressure, $p_0/p_{atm} \sim \mathcal{U}(0.85,1.15)$, random draws were performed to build the initial ensemble. A first ensemble, of size J=23 is used. This initial ensemble can be fitted to a normal distribution, $\mathrm{p_0/p_{atm}} \sim \mathcal{N}(1.05,0.073)$. The mean static pressure variation along the machine obtained with the forward model runs, between rotor and stator, and after stator will be used, allowing the prediction of the corrected compressor map (static-to-total) and the static pressure at plane 2. The used model error is estimated locally, using the comparison between a fine mesh and the medium mesh results on a baseline case.

The algorithm is only given an experimental observation at plane 4 (outlet of stage), $\mathrm{p_{s4}/p_0}$, with its due uncertainty, allowing the experimental measurement available at plane 2, $\mathrm{p_{s2}/p_0}$, to be used for the methodology validation. The obtained result is presented in Figure with the posterior update (light blue) of the inlet total pressure for a design point of interest (a) and the obtained corrected static-to-total compressor map for the H25 compressor stage (b).

From Figure 6 (a), it can be noticed that the update from the prior believe, $\mathrm{p_0/p_{atm}} \sim \mathcal{N}(1.05,0.073)$, about the inlet total pressure does not change significantly, being the posterior, $\mathrm{p_0/p_{atm}} \sim \mathcal{N}(1.06,0.052)$, shifted from the atmospheric pressure. Looking at Figure 6 (b), it seems that the estimation of the corrected compressor map is between the CFD scatter results (in a medium mesh) and the experimental data, underestimating the pressure ratios that the compressor has shown to achieve experimentally. This underestimation of the machine pressure ratio, $\mathrm{p_{s4}/p_0}$, can be related to the posterior inlet total pressure result, which overestimates the inlet total

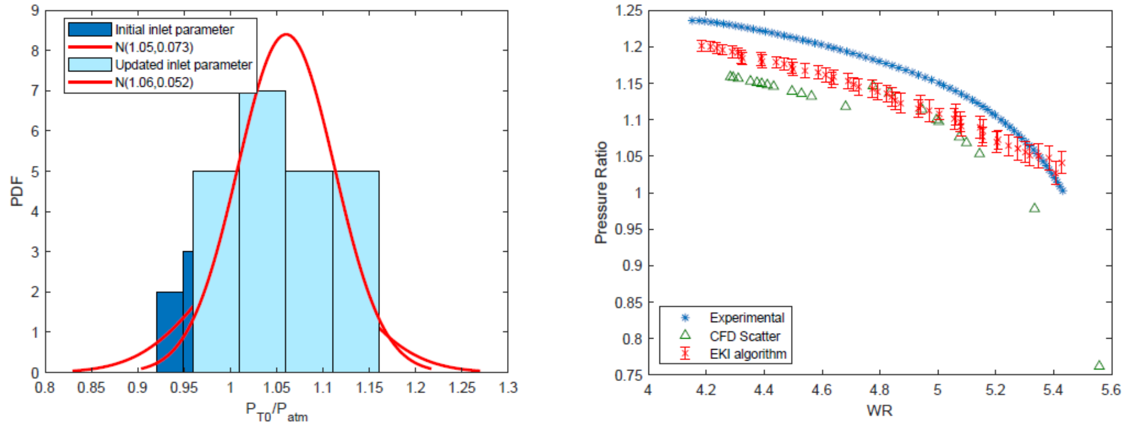

(a) Inlet Total Pressure Prior and Posterior

(b) Corrected Compressor map obtained with EnKF Inversion

Figure 6 - Mean Pressure 1D approach results obtained with EnKF Inversion using 23 CFD simulations to build the initial ensemble

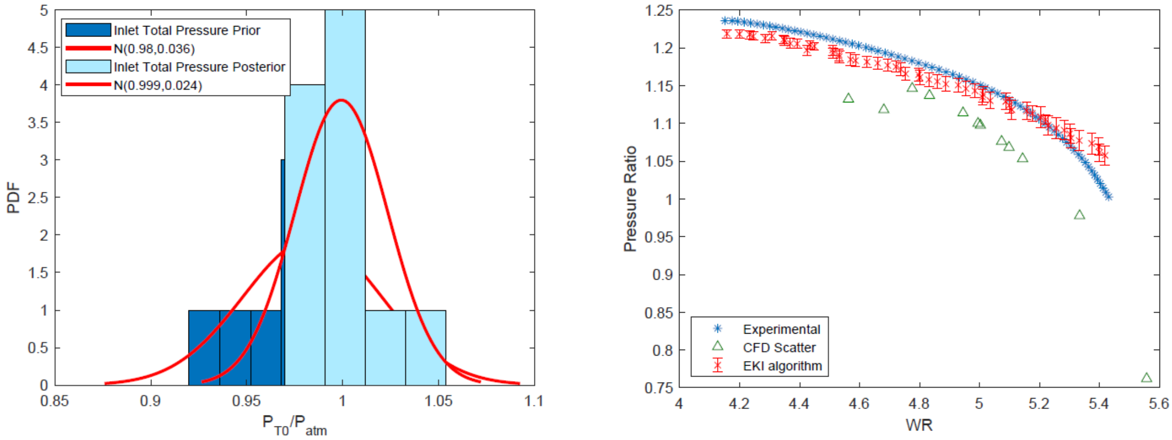

(a) Inlet Total Pressure Prior and Posterior

(b) Corrected Compressor map obtained with EnKF Inversion

Figure 7 - Mean Pressure 1D approach results obtained with EnKF Inversion using 12 CFD simulations to build the initial ensemble

pressure with respect to a reference atmospheric pressure, p_0/p_{atm}.

With the aim of improving the prediction of the compressor map, a second ensemble was generated by refining the initial 23 CFD into a more informative prior, that is fitted to a normal distribution around the atmospheric pressure $p_0/p_{atm} \sim \mathcal{N}(0.98,0.036)$. On one hand, this regularizes the inverse problem making it more prior bounded since the experimental observations are taken with a value of inlet pressure around atmospheric conditions. On the other hand, this more informative prior is constituted with less ensemble members since no extra CFD computations are to be performed, which by itself leads to worse algorithm performance.

Similarly to before, the obtained results with this second initial ensemble are presented below in Figure 7 with the posterior update (light blue) distribution for the inlet total pressure (a) and the obtained corrected static-to-total compressor map for the H25 compressor stage (b).

Looking firstly at Figure 7 (a), the posterior update for the inlet total pressure is presented in light blue. The posterior ensemble matches a normal distribution $p_0/p_{atm} \sim \mathcal{N}(1,0.023)$, meaning a distribution around the reference atmospheric value and with a standard deviation that is of the order of magnitude of atmospheric pressure fluctuations. This result is very interesting and shows a classical Bayes theorem result, a prior belief is updated and gives a posterior that is connected to the prior belief, but gets updated by new information, making it a more reliable result.

Going to the analysis of Figure 7 (b), the capacity of statistical inference and this methodology are in full display. The algorithm is capable of building a good corrected compressor map, just from a few CFD simulations in a medium level mesh and experimental observations at multiple working points, that is very close to the observed pressure ratios, except for higher mass flows where it shows a slight overestimation of performance.

The algorithm employed also gives as a result a belief of what is the static pressure ratio at plane 2 (after the rotor), which is used for validation and closes the methodology proposed. The validation logic used for this case, verifies if the experimental result, not given to the algorithm, is inside the pdf obtained by the algorithm update at plane 2, thus validating it. Figure 8 presents the prior "design space" occupied by the ensemble CFD scatter (red), the algorithm update result (black) given only an outlet experimental observation (blue) and the experimental observation at plane 2 (green).

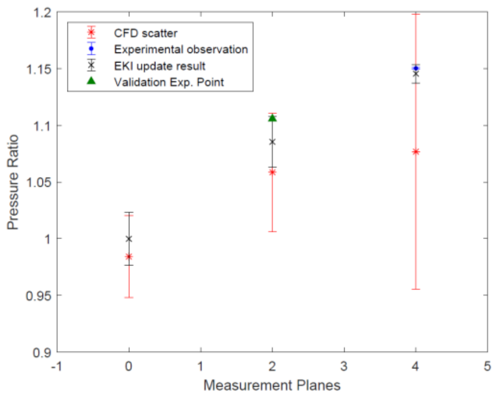

Figure 8 - Methodology validation with experimental data at measurement plane 2

The pressure ratios obtained at the various measurement planes with the algorithm employed, have a lower, more physical interval value, being plane 0 (the initial ensemble) made of smaller variations around the atmospheric reference pressure, for example. Looking at measurement plane 4, it can be noted how the algorithm reacts to the experimental observation given, updating the ensemble towards it, with a distribution that includes it.

It can be visually inferred that the experimental observation of the pressure ratio at plane 2, despite not given to the algorithm, is inside the obtained result, serving as a validation of the methodology and demonstrating the concept of Bayesian inference applied to turbomachinery, showing its capacity to retrieve the compressor map with limited data, but, in this case, also predict the behaviour of the machine in the inter-row plane.

CONCLUSIONS

In this work, the concept of a new hybrid experimental technique methodology, that couples numerical modelling with experimental data using data assimilation performed by Bayesian inference is presented. It aims at reducing the number of required probes to characterize a machine, leading to less costs and lower probe intrusiveness on the flow while maintaining fidelity results.

A bibliographic research into the topic of Bayesian statistics and data assimilation was performed and various methods were found suitable for this new methodology. The Ensemble Kalman Filter for inverse problems (Iglesias et al., 2013) was chosen due to its gradient free, low computational cost and literature promising results in fluid mechanics problems.

Focus was given on building the compressor map, providing experimental data taken at the outlet of the stator, and validating the results with data taken between rotor and stator. This approach revealed that the algorithm is not only able to retrieve the compressor map, but also predict the inter-row pressure ratio, proving the capability of the methodology to reduce experimental measurements required to characterize the stage. The influence of the prior used was analysed, being a second run of the methodology with a more informative prior performed, obtaining an improved result.

Finally, it is important to remark the room for improvement of the methodology, from increasing the ensemble size, to performing more iterations of the methodology, but, more importantly, optimizing the experimental measurements selected for the data assimilation process along the flow field domain.

REFERENCES

Apte, A., Hairer, M., Stuart, A. M., & Voss, J. (2007). Sampling the posterior: An approach to non-Gaussian data assimilation. *Physica D: Nonlinear Phenomena*, *230*(1–2), 50–64. https://doi.org/10.1016/j.physd.2006.06.009

Aschenbruck, J., Hauptmann, T., & Seume, J. R. (2015). Influence of a multi-hole pressure probe on the flow field in axial-turbines. *11th European Conference on Turbomachinery Fluid Dynamics and Thermodynamics, ETC 2015*, 1–13.

Babin, C., Ottavy, X., & Dumas, M. (2020). Numerical Characterization of a HP compressor stage equipped with a closed shrouded stator cavity. *ASME Turbo Expo 2020*, 1–13.

Bannister, R. N. (2017, January 1). A review of operational methods of variational and ensemble-variational data assimilation. *Quarterly Journal of the Royal Meteorological Society*. John Wiley and Sons Ltd. https://doi.org/10.1002/qj.2982

Dwight, R. P. (2014). Bayesian inference for data assimilation using Least-Squares Finite Element methods. *IOP Conference Series: Materials Science and Engineering*, *10*(1). https://doi.org/10.1088/1757-899X/10/1/012224

Evensen, G. (2003). The Ensemble Kalman Filter: Theoretical formulation and practical implementation. *Ocean Dynamics*, *53*(4), 343–367. https://doi.org/10.1007/s10236-003-0036-9

Evensen, G. (2010). *Data assimilation: The ensemble kalman filter*. *Data Assimilation: The Ensemble Kalman Filter*. https://doi.org/10.1007/978-3-540-38301-7

Ide, K., & Ghil, M. (1998). Extended Kalman filtering for vortex systems. Part II: Rankine vortices and observing-system design. *Dynamics of Atmospheres and Oceans*, *27*(1–4), 333–350. https://doi.org/10.1016/s0377-0265(97)00017-1

Iglesias, M. A., Law, K. J. H., & Stuart, A. M. (2013). Ensemble kalman methods for inverse problems. *Inverse Problems*, *29*(4). https://doi.org/10.1088/0266-5611/29/4/045001

Jardak, M., Navon, I. M., & Zupanski, M. (2010). Comparison of sequential data assimilation methods for the Kuramoto-Sivashinsky equation. *International Journal for Numerical Methods in Fluids*, *62*(4), 374–402. https://doi.org/10.1002/fld.2020

Lorenc, A. C. (2003). The potential of the ensemble Kalman filter for NWP - A comparison with 4D-Var. *Quarterly Journal of the Royal Meteorological Society*, *129*(595 PART B), 3183–3203. https://doi.org/10.1256/qj.02.132

Lorenz, E. N. (1963). Deterministic Nonperiodic Flow. *Journal of the Atmospheric Sciences*. https://doi.org/10.1175/1520-0469(1963)020<0130:dnf>2.0.co;2

Marzouk, Y. M., & Najm, H. N. (2009). Dimensionality reduction and polynomial chaos acceleration of Bayesian inference in inverse problems. *Journal of Computational Physics*, *228*(6), 1862–1902. https://doi.org/10.1016/j.jcp.2008.11.024

Menter, F. R. (1994). Two-equation eddy-viscosity turbulence models for engineering applications. *AIAA Journal*. https://doi.org/10.2514/3.12149

Penenko, V. V. (2009). Variational methods of data assimilation and inverse problems for studying the atmosphere, ocean, and environment. *Numerical Analysis and Applications*, *2*(4), 341–351. https://doi.org/10.1134/S1995423909040065

Sakov, P., & Oke, P. R. (2008). A deterministic formulation of the ensemble Kalman filter: An alternative to ensemble square root filters. *Tellus, Series A: Dynamic Meteorology and Oceanography*, *60 A*(2), 361–371. https://doi.org/10.1111/j.1600-0870.2007.00299.x

Sanders, C., Terstegen, M., Hölle, M., Jeschke, P., Schönenborn, H., & Fröbel, T. (2017). Numerical studies on the intrusive influence of a five-hole pressure probe in a high-speed axial compressor. *Proceedings of the ASME Turbo Expo*, *2*A-*2017*, 1–12. https://doi.org/10.1115/GT201763399

Sousa, J., García-Sánchez, C., & Gorlé, C. (2018). Improving urban flow predictions through data assimilation. *Building and Environment*, *132*(January), 282–290. https://doi.org/10.1016/j.buildenv.2018.01.032

Sousa, J., & Gorlé, C. (2019). Computational urban flow predictions with Bayesian inference: Validation with field data. *Building and Environment*, *154*, 13–22. https://doi.org/10.1016/j.buildenv.2019.02.028

Stordal, A. S., Karlsen, H. A., Nævdal, G., Skaug, H. J., & Vallès, B. (2011). Bridging the ensemble Kalman filter and particle filters: The adaptive Gaussian mixture filter. *Computational Geosciences*, *15*(2), 293–305. https://doi.org/10.1007/s10596-010-9207-1

Wikle, C. K., & Berliner, L. M. (2007). A Bayesian tutorial for data assimilation. *Physica D: Nonlinear Phenomena*, *230*(1–2), 1–16. https://doi.org/10.1016/j.physd.2006.09.017

Zhang, X.-L., Michelén-Ströfer, C., & Xiao, H. (2019). Regularization of Ensemble Kalman Methods for Inverse Problems, (October), 1–40.